

Spectroscopic Properties, Excitation, and Electron Transfer in an Anionic Water-Soluble Poly(fluorene-*alt*-phenylene)-perylene-3,4,9,10-tetracarboxylic diimide Copolymer

Ana T. Marques,^{*,†,‡} Hugh D. Burrows,[†] J. Sérgio Seixas de Melo,[†] Artur J. M. Valente,[†] Lúcia L. G. Justino,^{†,§} Ullrich Scherf,[‡] Eduard Fron,^{||} Susana Rocha,^{||} Johan Hofkens,^{||} Edward W. Snedden,[⊥] and Andrew P. Monkman[⊥]

[†]Department of Chemistry, University of Coimbra, P3004-535 Coimbra, Portugal

[‡]Macromolecular Chemistry Group, University of Wuppertal, D-42097 Wuppertal, Germany

[§]Centro de Neurociências e Biologia Celular, Universidade de Coimbra, 3004-517 Coimbra, Portugal

^{||}Department of Chemistry, University of Leuven, Celestijnenlaan 200F, 3001 Heverlee, Belgium

[⊥]Organic Electroactive Materials Group, Department of Physics, Durham University, DH1 3LE, United Kingdom

Supporting Information

ABSTRACT: An anionic fluorene-phenylene poly{1,4-phenylene-[9,9-bis(4-phenoxy-butylsulfonate)]fluorene-2,7-diyl}-based copolymer containing on-chain perylene-3,4,9,10-tetracarboxylic diimide (PDI) chromophoric units, PBS-PFP-PDI, was synthesized and its photophysical properties studied as aggregates and isolated chains in water and dioxane/water (1:1) solution. UV-vis and emission spectroscopy measurements, time-correlated single photon counting, and wide field imaging have been employed to investigate the excited-state behavior of the PBS-PFP-PDI copolymer, including the effect of environment on the energy and electron transfer to the on-chain PDI chromophore. Although the Förster overlap integral is favorable, no evidence is found for intramolecular singlet excitation energy transfer in isolated copolymer chains in solution. Fluorescence is suggested to involve an interchain process, thus revealing that isolated copolymer chains in solution do not undergo efficient intramolecular energy transfer. However, quenching of the PBS-PFP excited state by PDI is observed in aqueous media and ultrafast pump-probe studies in water or dioxane-water solutions show that electron transfer occurs from the phenylene-fluorene units to the PDI. The extent of electron transfer increases with aggregation, suggesting it is largely an interchain process. The interaction of the negatively charged PBS-PFP-PDI copolymer with the positively charged surfactant hexadecyltrimethylammonium bromide (CTAB) in solution has also been studied. The copolymer PBS-PFP-PDI aggregates with the surfactant already at concentrations below the critical micelle concentration (cmc) and the nonpolar environment allows intermolecular energy transfer, observed by the weak emission band located at 630 nm that is associated with the emission of the PDI chromophore. However, the fact that the PDI photoluminescence (PL) lifetime (~ 1.4 ns) obtained in the presence of CTAB is considerably shorter than that of the nonaggregated chromophore (~ 5.4 ns) suggests that even in this case there is considerable PL quenching, possibly through some charge transfer route. The increase of the PBS-PFP-PDI photoluminescence intensity at surfactant concentrations above the cmc indicates deaggregation of polyelectrolyte within the initially formed polyelectrolyte-surfactant aggregates.

Energy transfer C₁₆TAB, nonpolar environment

$^1\text{PBS-PFP}^*-\text{PDI}$ \longrightarrow $\text{PBS-PFP}-^1\text{PDI}^*$
(700 - 900 nm) (650 - 900 nm)

Electron transfer polar solvent

$^1\text{PBS-PFP}^*-\text{PDI}$ \longrightarrow $\text{PBS-PFP}^{++}-\text{PDI}$
(500 - 550 nm)
 $\text{PBS-PFP} \longrightarrow \text{PDI}^{++}$
(650 nm)

INTRODUCTION

Conjugated polyelectrolytes (CPEs) are π -conjugated polymers with polar and ionic solubilizing side chains that are covalently bound to the π -conjugated main chain.¹⁻⁴ The applications of CPEs include their use as buffer and emissive materials for inkjet printed layers,⁵ light emitting displays (LEDs),⁶⁻⁸ light emitting electrochemical cells (LECs),^{9,10} and fluorescence sensors for chemical or biological analytes,^{1,11-17} as well as their use as electron transport or injection layers of electronic devices¹⁸⁻²⁰ and photovoltaic cells.^{21,22}

An important class of CPEs involves fluorene-based materials that combine advantages, such as a high fluorescence quantum yield of the blue emission, with the ability to change the electronic properties through modification of the polymer structure. The incorporation of on-chain chromophoric units introduces the possibility of excitation energy transfer (Förster resonance energy transfer, FRET).²³⁻²⁶ However, CPEs based

Received: January 3, 2012

Revised: May 2, 2012

Published: May 3, 2012

on relatively rigid polymers, as is the case of polyfluorenes (PFs), generally show a low solubility in water with the tendency to form clusters. To overcome this solubility problem in aqueous solution, either organic cosolvents^{17,27,28} or surfactants ("surfactochromicity")^{29–33} have often been employed. The addition of surfactants often leads to a deaggregation of the copolymer chains, thus increasing the fluorescence quantum yield of the polymer.

By incorporating molecular moieties with different HOMO/LUMO bandgaps, the polymer emission can be tuned across the visible spectrum, providing excellent prospects for the polymer's application in various areas of optoelectronics.^{34–37} We have previously shown that it is possible to observe on-chain singlet excited state energy transfer from phenylene-fluorene to porphyrin units in an anionic conjugated polyelectrolyte.³⁸ We have chosen to extend this to the perylenediimide (PDI) moiety, incorporated in the PF main chain. The PDI moiety possesses a lower energy optical transition than polyfluorene, has a compact and electron deficient core with high thermal and photo stability, a high absorption coefficient, and a fluorescence quantum yield close to unity.^{39–41} This allows the possibility of both electronic energy transfer and charge transfer to the PDI chromophore.^{42,43}

Color tuning in organic conjugated polymers (CP) through Forster resonance energy transfer involves a dipole–dipole interaction between two different on-chain or side-chain moieties.^{44,45} Energy transfer may also involve an exchange mechanism (Dexter), following exciton hopping. In donor–acceptor polymers, the transfer mechanism normally includes excitation diffusion within the donor, followed by nonradiative transfer from the donor to the acceptor moieties.⁴⁶ However, FRET is not restricted to nonradiative transfer from a donor in an excited singlet state to a ground-state acceptor and can also occur between excited donor and acceptor molecules with different spin multiplicities. Hence, the transfer of excitation energy from a chromophore residing in the first excited singlet state to another chromophore, either in its first excited singlet or triplet state, to give the corresponding higher excited states of the acceptor molecule is potentially possible. These processes are also known as singlet–singlet or singlet–triplet annihilation and represent competing energy transfer (ET) pathways.^{35,45–50}

Furthermore, the efficiency of energy transfer also depends on other competing decay channels, such as electron transfer. Excited states and charge separated species show marked differences in their dependence upon solvent polarity, and it is of considerable interest to develop an understanding of the factors which control this for a particular system.

In this contribution, we discuss the spectroscopic and photophysical properties of an anionic fluorene-phenylene CPE copolymer with on-chain perylenediimide units both in solution and in film. The study also reports the effect of adding an oppositely charged surfactant to copolymer solutions. The results are compared with the behavior of structurally related, uncharged copolymers containing identical main chain dye units.^{37,45}

■ EXPERIMENTAL SECTION

Synthesis of Materials. For the preparation of the copolymer PBS-PFP-PDI, a mixture of 2,7-dibromo-9,9-bis(4-sulfonylbutoxyphenyl)fluorene (0.783 g, 0.95 mmol), *N,N'*-bis(4-bromophenyl)-1,6,7,12-tetra(phenoxyl)-perylene-3,4,9,10-

tetracarboxydiimide, PDI (0.053 g, 0.05 mmol), 1,4-benzenedi-boronic acid (0.166 g, 1 mmol), Pd(PPh₃)₄ (50 mg), Na₂CO₃ (1.0 g, 9.4 mmol) in 50 mL of toluene, 5 mL of water, and 5 mol of butanol was reacted for 4 days under reflux. The aqueous layer was washed with chloroform and concentrated to dryness.⁴⁷ The residue was redissolved in a mixture of water and THF 50% (v/v), and then purified by dialysis using a membrane with a cutoff of 3500 g·mol⁻¹. On the basis of the monomer/PDI ratio in the starting reaction mixture, the copolymer is expected to contain on average 5% PDI units. The total yield of the copolymer PBS-PFP-PDI was 374 mg (47%). ¹NMR (400 MHz, d-THF 50% D₂O, ppm) 8.18 (ar-H PDI), 7.80–7.00 (ar-H PDI and ar-H fluorene), 4.17 (γ –CH₂), 3.07 (α –CH₂), 2.08 (β , δ –CH₂). FTIR 1652, 1662, and 1698 (sh) cm⁻¹ for the imide groups and 1507.5, 1578, and 1600 cm⁻¹ for the perylene skeleton. GPC (NMP/LiBr, UV detection 360 nm) *M*_w = 2100 g·mol⁻¹, *M*_w/*M*_n = 1.61 gave a rather small *M*_w value of only 2100 g/mol. This value seems considerably underestimated as a result of polar interactions of the conjugated polyelectrolyte with the column material (as can be seen by the cutoff of the dialysis membrane at 3500 g/mol).^{51,52} For the homopolymer PBS-PFP without on-chain PDI units, a molecular weight *M*_n of ca. 6500 g·mol⁻¹ was determined.⁵¹ Quite similar values are expected for the related copolymers containing on-chain PDI units.

The syntheses of monomer PDI³⁷ and PBS-PFP⁴⁵ monomers were described previously.

Steady State Measurements. The measurements were recorded in water and in a (1:1) dioxane–water (v/v) mixture. Dioxane of spectroscopic grade and Milli-Q water was used. To ensure almost complete dissolution of the copolymer, solutions were stirred overnight. The cationic surfactant hexadecyltrimethylammonium bromide (CTAB) was purchased from Sigma-Aldrich and used without further purification. Fluorescence quantum yields were measured using quinine sulfate in 0.5 M sulfuric acid (ϕ_F = 0.546) and rhodamine 6G in ethanol (ϕ_F = 0.94) as references.⁵³ Absorption spectra were recorded using a Shimadzu UV-2100 spectrophotometer with a minimum spectral resolution of 0.2 nm. For the steady-state measurements, fluorescence spectra were recorded with a Horiba-Jobin-Ivon SPEX Fluorog 3-22 spectrometer and were corrected for the instrumental response of the system.

Nanosecond and Picosecond TCSPC Experiments. Fluorescence decays on the nanosecond time scale were measured using a home-built time-correlated single photon counting (TCSPC) apparatus as described elsewhere,^{54,55} except that a Horiba-JI-IBH NanoLED, λ_{exc} = 460 nm, was used as the excitation source. Picosecond time-resolved fluorescence measurements were performed using a home-built picosecond TCSPC apparatus, in which the excitation source consists of a picosecond Spectra Physics mode-lock Tsunami laser (Ti:sapphire) model 3950 (repetition rate of about 82 MHz, tuning range 700–1000 nm), pumped by a Millennia Pro-10s, frequency-doubled continuous wave (CW), diode-pumped, solid-state laser (λ_{em} = 532 nm). A harmonic generator model GWU-23PS (Spectra-Physics) is used to produce the second and third harmonic from the Ti:sapphire laser exciting beam frequency output. The samples were measured with excitation at 392 nm, and the horizontally polarized output beam from the GWU (second harmonic) was first passed through a ThorLabs depolarizer (WDPOL-A) and next through a Glan-Thompson polarizer (Newport 10GT04) in order to obtain vertical polarization. Emission collected in a

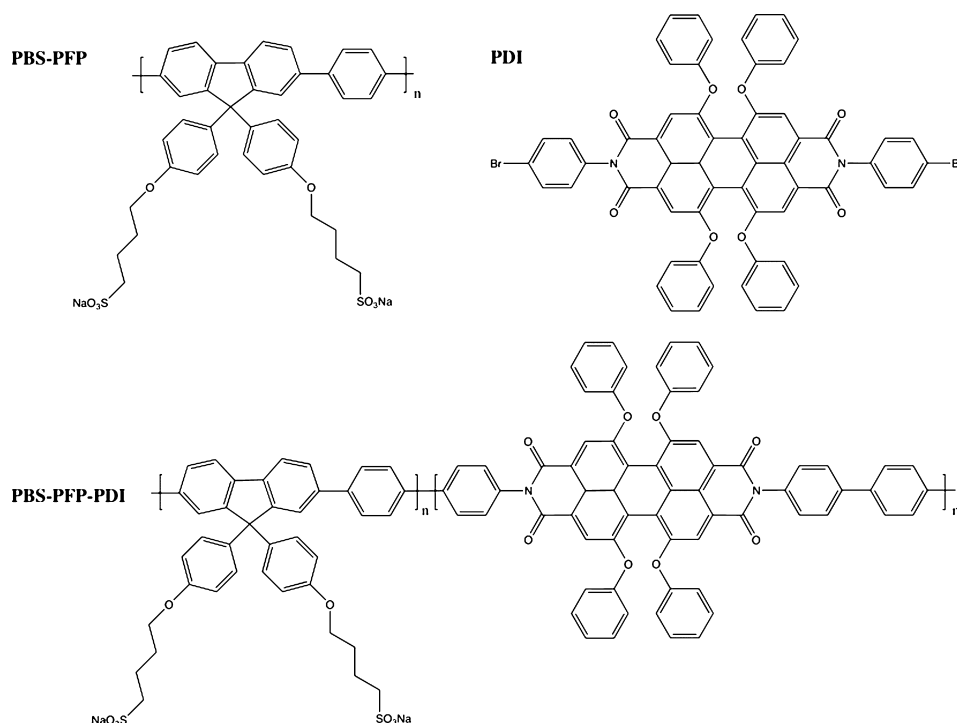


Figure 1. Chemical structures of the homopolymer PBS-PFP, the PDI monomer, and the copolymer PBS-PFP-PDI.

90° geometry and at the magic angle was detected through a double subtractive Oriel Cornerstone 260 monochromator by a Hamamatsu microchannel plate photomultiplier (R3809U-50). Signal acquisition and data processing were performed employing a Becker & Hickl SPC-630 TCSPC module. Fluorescence decays and the instrumental response function (IRF) were collected using 4096 channels in a 0.814 ps/channel scale, until 5×10^3 counts at maximum were reached. The full width at half-maximum (fwhm) of the IRF was about 22 ps and was highly reproducible with identical system parameters. A more detailed description of this equipment can be found in refs 56 and 57. The deconvolution of the fluorescence decays (ns and ps) was made with the modulating functions method implemented by G. Striker and is described given elsewhere.⁵⁸

Pump–Probe Measurements. Ultrafast spectroscopic measurements were made using a conventional femtosecond non-collinear pump–probe setup. 180 fs, 4 μ J, pulses of 100 kHz repetition rate at 1.60 eV were generated using a Coherent Mira900-f Ti:sapphire femtosecond oscillator in conjunction with a Coherent RegA 9000 laser amplifier. The output of this system was fed into a Coherent 9400-OPA, which was used to generate a single-wavelength output (390 nm) to pump, with a white-light supercontinuum (470–1000 nm) used as a probe. The variable delay between pulses was controlled by means of a motorized stage, with the polarization of both pulses orientated at 54.7° (magic angle) to each other using a variable quarter-waveplate. Spectral components in the probe were isolated using a monochromator (Bentham M300) incorporating visible and IR gratings, with the relative transmission change $\Delta T/T$ of the probe beam measured using a Si photodetector and lock-in amplifier referenced to the mechanically chopped pump beam.

Single Molecule Wide-Field Imaging and Analysis. Wide field fluorescence microscopy was performed on an inverted microscope (Olympus IX-71) equipped with a TIRF oil objective (60 \times , NA1.6, Olympus) and a cooled Electron

Multiplying-CCD (ImagEM, Hamamatsu). The fluorene-phenylene moiety was excited with 0.1–0.5 kW/cm² from a 375 nm laser (SpectraPhysics), while PDI subunits were excited with 1–5 kW/cm² from a 561 nm (Jive, Cobolt) diode pumped solid state laser. The laser lines were combined using a 505 dichroic (505DCLP Chroma Technology, Inc.) and further guided onto the sample through the same dichroic mirror (z561rdc Chroma Technology, Inc.). Emission from the PDI was collected through a 570 long pass and a 600/60 band filter (HQ570LP and HQ600/60, Chroma Technology, Inc.), while emission from the fluorene-phenylene units was collected via a 430 long pass filter (HQ430LP, Chroma Technology, Inc.). The images were acquired with a final maximum field of view of ca. 41 \times 41 μ m² (80 \times 80 nm² per pixel) with a frame rate depending on the excited fluorophore, more specifically, 5 Hz when exciting PDI and 0.5–0.33 Hz when exciting fluorene-phenylene.

Computational Details. The molecular structure of PBS-PFP-PDI was optimized at the DFT level without symmetry constraints using the GAMESS code.⁵⁹ The B3LYP (Becke three-parameter Lee–Yang–Parr)^{60,61} exchange correlation functional was employed, and due to the relative large size of the system, the 3-21G(d) basis sets were used for the expansion of the Kohn–Sham orbitals of all the atoms. The gradient threshold for geometry optimization was taken as 10^{−5} Hartree Bohr^{−1}. The reported DFT HOMO−1, HOMO, LUMO, and LUMO+1 energies correspond to the Kohn–Sham eigenvalues.

RESULTS AND DISCUSSION

Steady-State Measurements. The absorption and photoluminescence emission spectra of the PBS-PFP-PDI copolymer were recorded both in water and dioxane–water (1:1) mixture. The steady-state spectra in dioxane–water are shown in Figure 2. The spectral data observed for the PBS-PFP-PDI copolymer and the PBS-PFP homopolymer in the two solvents are summarized in Table 1.

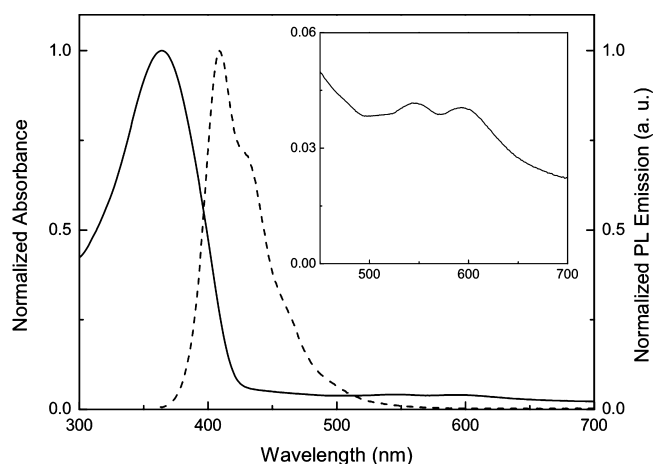


Figure 2. Absorption and emission spectra of the PBS-PFP-PDI copolymer in a (1:1) dioxane–water mixture. The inset depicts the 400–700 nm region of the PBS-PFP-PDI absorption shown in the main plot.

Table 1. Absorption and Emission Maxima (Collected at the PF Absorption Band) and Photoluminescence Quantum Yields of PBS-PFP-PDI and PBS-PFP

	water			(1:1) dioxane–water		
	abs. (nm)	emis. (nm)	Φ_F	abs. (nm)	emis. (nm)	Φ_F
PBS-PFP-PDI	369	424	0.08	360	409	0.55
PBS-PFP	386	426	0.06	375	413	0.52

The absorption spectra of PBS-PFP-PDI show an intense absorption band at 360 nm, characteristic of the poly(fluorene-*alt*-phenylene) backbone⁵¹ together with a very small absorbance in the 400–615 nm region associated with the incorporated on-chain PDI units.^{37,45} Considering the high molar extinction coefficient of PDI, the small absorbance value (ca. 4% when compared with the PF absorption band) mirrors a low degree of PDI incorporation (Figure 2). As has been reported for related systems,⁶² the use of the organic cosolvent is expected to minimize aggregation in solution. In particular, the blue shift in the emission maximum upon the addition of dioxane and the increase in the fluorescence quantum yield (Table 1) suggest the existence of isolated copolymer chains in the dioxane–water mixture.^{62,63}

The emission spectra of the copolymer in both solvents (excitation at 360 nm) shows only fluorescence arising from PF units, although, as depicted in Figure 4, there is a good spectral overlap between the homopolymer PBS-PFP emission and PDI absorption. Upon direct excitation into the PDI unit at 540 nm, no emission from the PDI chromophore could be detected, suggesting a very efficient nonradiative deactivation of the PDI excited state in these solvents, as has been reported for related systems.⁴⁵ The photoluminescence quantum yield (PLQY) of the PDI molecule in dioxane is close to unity,⁶⁴ whereas this value drops to 0.06 in the (1:1) water–dioxane mixture. This indicates the presence of new deactivation pathways (e.g., a more efficient radiationless decay) of the PDI local excited state, due to the water content in the solution, and/or aggregation.⁶⁵

For the copolymer in dioxane–water, the fluorescence quantum yield was found to be 0.55; this value drops to 0.08

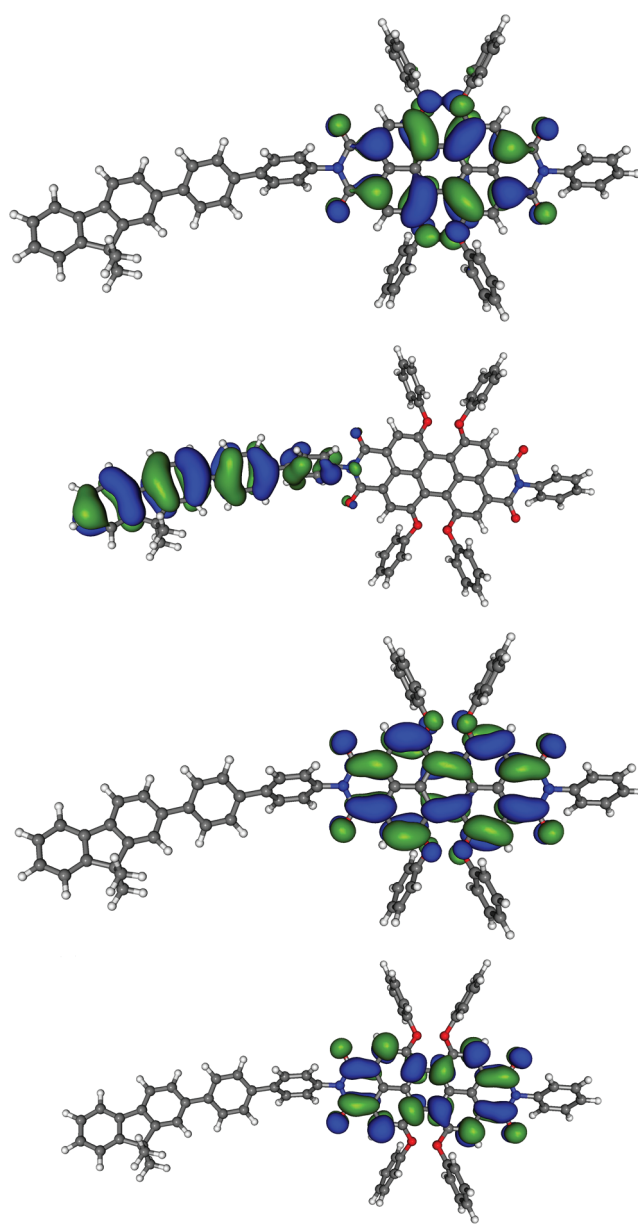


Figure 3. Contour plots of the HOMO–1, HOMO, LUMO, and LUMO+1 orbitals of PDI-phenylene-fluorene model oligomers as calculated at the B3LYP/3-21G* level. HOMO–1 = –5.46 eV, HOMO = –5.20 eV, LUMO = –2.84 eV, and LUMO+1 = –1.58 eV.

in water, suggesting again the presence of additional deactivation pathways. This is likely to be associated with aggregation, which is further supported by a 15 nm red shift of the emission maxima when compared to the water–dioxane mixture.⁶² Although aggregation is likely to be affected by both counterion and ionic strength,⁶⁶ only the sodium salt of the conjugated polyelectrolyte was studied, and at the low overall polymer concentrations used (<1 mM), ionic strength effects are not expected to be important.

DFT calculations illustrate that the PDI unit is not electronically coupled to the PFP backbone (Figure 3) and that electronic energy transfer between the two parts can occur via dipole–dipole interaction (Förster energy transfer). This is in agreement with previous studies reported by Beljonne et al. on polyindenofluorenes end-capped with a perylene derivative,

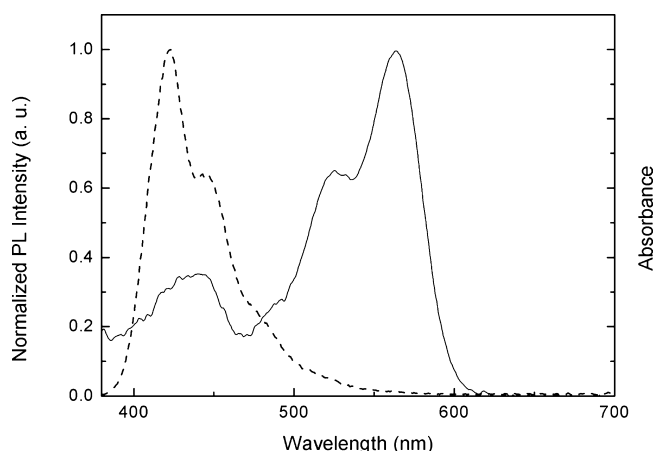


Figure 4. Spectral overlap between homopolymer PBS-PFP emission and PDI absorption.

which showed rather slow on-chain energy transfer to the perylene dye end-caps but fast interchain energy transfer.⁶⁷

The Förster radius (R_0) for PBS-PFP and PDI was calculated from the spectral overlap using eq 1.^{68,69}

$$J(\lambda) = \int_0^\infty F_D(\lambda) \epsilon_A(\lambda) \lambda^4 d\lambda \quad (1)$$

We used the spectral overlap between the PBS-PFP polymer and the PDI chromophore, together with the PDI molar extinction coefficient and the donor fluorescence yield, to calculate the Förster radius (R_0), which is the distance at which energy transfer occurs with 50% efficiency.^{68,69} This leads to a Förster radius of 47 Å. On the basis of the dependence of k_{ET} (eq 2) with the distance between the donor and acceptor (r)⁷⁰

$$R_0 (\text{Å}) = 0.211 [k^2 n^{-4} \Phi_D J(\lambda)]^{1/6} \quad (2)$$

with $\tau_D = 515 \text{ ps}$ ⁶⁹ and $R_0 = 47 \text{ Å}$, we obtain values for $k_{ET} = 2.06 \times 10^9 \text{ s}^{-1}$ ($r = 47 \text{ Å}$) and $4.72 \times 10^{11} \text{ s}^{-1}$ (van der Waals radius, $r = 19 \text{ Å}$). From the fluorescence decay measurements, the decay time potentially associated with the energy transfer process (which can also include or be associated with conformational relaxation processes)⁶⁷ leads to a rate constant of $1.67 \times 10^{10} \text{ s}^{-1}$, vide infra. More details on the distance

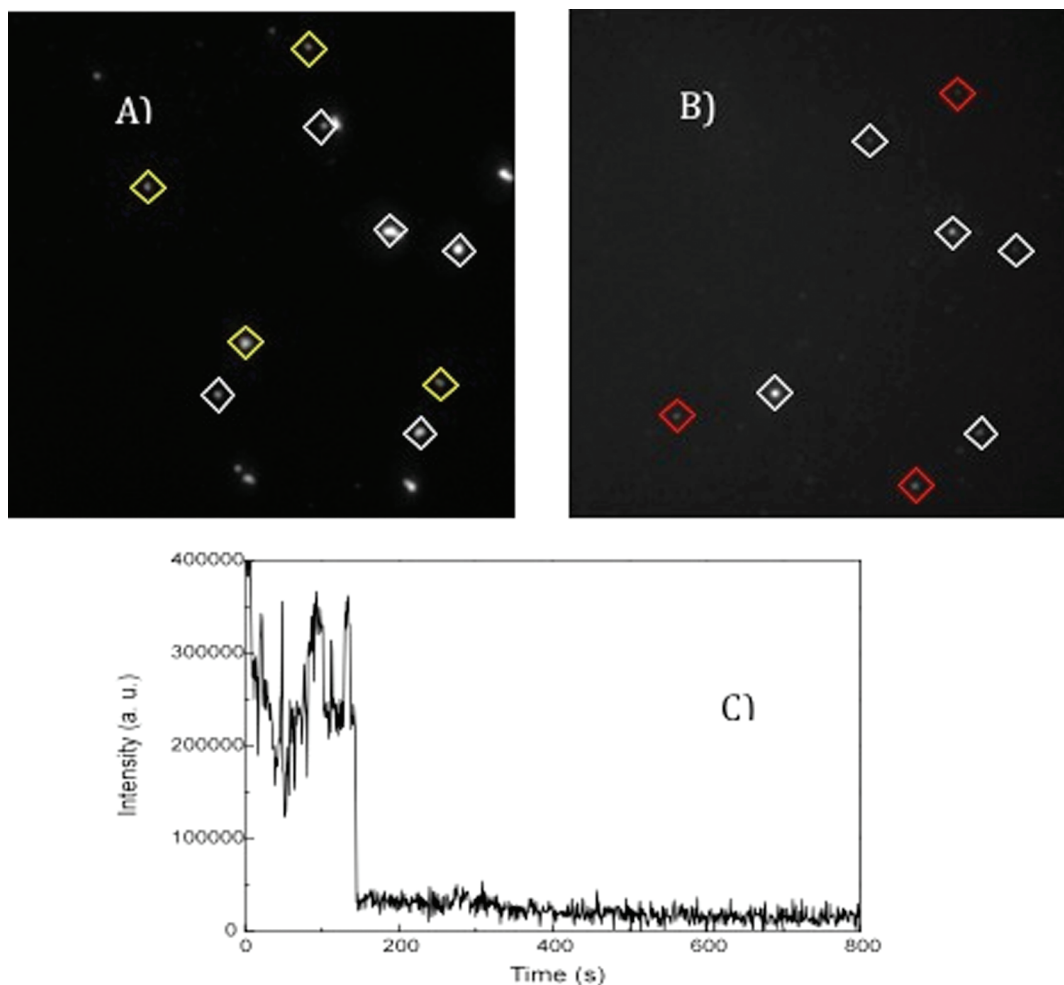


Figure 5. Wide-field images and fluorescence intensity trajectory of individual PBS-PFP-PDI copolymers dispersed in a PVA film. (A) Wide-field image recorded with 375 nm excitation light. The PBS-PFP units are absorbing moieties, and fluorescence is emitted by either PF (yellow spots) or PDI incorporated in the copolymer chain (white spots). (B) Wide-field image recorded with 561 nm excitation light of the same area as part A. The PDI units are the absorbing and emitting species in this image; the red spots show “isolated” PDI spots without a corresponding PBS-PFP spot in part A. The white spots are PDI chromophores unambiguously attached to PBS-PFP. Part C represents an example of a PBS-PFP-PDI copolymer containing one PDI chromophore.

dependence of the rate of energy transfer are given in the Supporting Information.

Distances ranging from 20 to 40 Å have previously been found for related fluorene containing macromolecules.^{34,45,70–73} The fact that no energy transfer is observed through PDI emission, although the calculations indicate this possibility, suggests that an alternative photophysical pathway (such as charge transfer from polymer to PDI⁴⁵) exists with isolated CPE chains in the (1:1) dioxane–water solution. Although no attempt was made to look for intermolecular energy transfer between PBS-PFP and PDI molecules in solution due to solubility problems, as noted above, it is known that it does occur from interchain studies on polyindeno-fluorenes end-capped with a perylene derivative.⁶⁷

Single-Molecule Wide Field Imaging. In order to determine the PDI fraction that is actually incorporated in the PBS-PFP-PDI single chain, wide field imaging experiments were employed.⁷³ For this, wide-field images and fluorescence intensity trajectories of individual polymer chains dispersed in a PVA film were recorded, as in the work described by Fron et al.⁴⁵ and Delport et al.⁷⁴ Two excitation lasers were used, 375 and 561 nm, to selectively excite the PBS-PFP and PDI units. Upon excitation of the PBS-PFP moieties, emission from PDI units was observed, indicating that excitation energy transfer does take place from PBS-PFP to the PDI as energy donor and acceptor, respectively.⁷⁵ This also suggests that this process occurs more efficiently in a solvent free environment possibly associated with changes in both polarity and the polymer chain conformation (folding) (Figure 5). The single molecule wide field technique was also used to estimate the number of incorporated PDI units within a single polymer chain. The emission occurring from the polymer chains was first visualized upon 375 nm excitation and the observed area selected. A movie was then recorded of this area with 561 nm excitation, until all the molecules were photobleached. Using this, it was possible to identify the PBS-PFP-PDI copolymers and build the copolymer fluorescence intensity time trajectories. Following this, a control movie was made with 375 nm excitation to check if all the copolymers were still present and whether the PBS-PFP units were still emitting (Figure 5). On the basis of these measurements, the exact number of PDI units present in each copolymer could be determined. The resulted histogram is depicted in Figure 6, and the majority of the observed copolymers show the presence of one PDI subunit in the PBS-PFP-PDI molecule.

The number of intensity levels observed can be assumed to correspond to the number of PDI units. On the basis of the wide-field experiments, 272 molecules were visualized with 375 nm excitation, of which 63% also reveal emission when excited with 561 nm wavelength (copolymer fraction that contains on-chain PDI chromophores) and 37% do not (PBS-PFP fraction).

Time-Resolved Fluorescence Measurements. For a better understanding of the excited-state behavior of the PBS-PFP-PDI copolymer, time-resolved fluorescence experiments^{76,77} were performed in the two solvent systems studied and collected at the copolymer emission maxima (see Tables 2 and 4). The fluorescence decays were best fitted with double- and triple-exponential decay laws according to eqs 3 and 4

$$I_{\lambda}(t) = a_{i1}e^{-t/\tau_1} + a_{i2}e^{-t/\tau_2} \quad (3)$$

and

$$I_{\lambda}(t) = a_{i1}e^{-t/\tau_1} + a_{i2}e^{-t/\tau_2} + a_{i3}e^{-t/\tau_3} \quad (4)$$

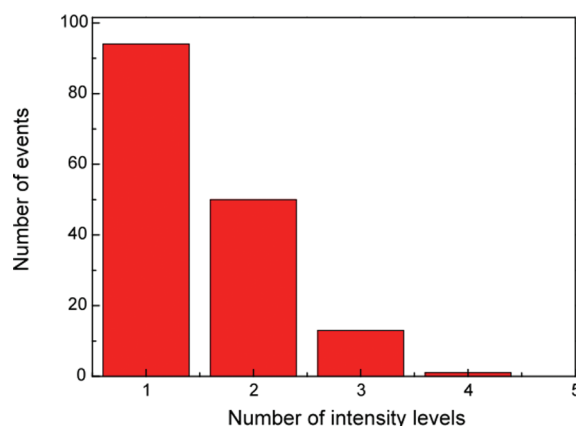


Figure 6. Number of fluorescence intensity levels corresponding to the number of PDI units in single PBS-PFP copolymer chain.

where a_{ij} ($j = 1, 2, 3$) are the pre-exponential factors and τ_i are the decay times (with $i = 1$ for $\lambda_{em} = 411$ nm and $i = 2$ for $\lambda_{em} = 635$ nm for the PBS-PFP-PDI with maximum CTAB concentration). The data are summarized in Table 2 and Figure 7, and the additional decay profile of homopolymer PBS-PFP is given in the Supporting Information. The physical meaning of the different components will be the focus of the discussion presented below.

For the model PDI compound in dioxane, a monoexponential decay was obtained with a lifetime of 5.65 ns, which is close to the value previously reported for PDI compounds, 5–6 ns.⁷⁴ For the PBS-PFP-PDI copolymer, the fluorescence decays observed at the polyfluorene emission maximum were fitted with sums of two or three discrete exponential functions, as has previously been found for polyfluorene (PF) based polyelectrolytes.^{71,78}

As discussed elsewhere,^{43,45,79,80} the fast component observed is believed to include contributions from both energy migration (either on-chain or interchain in water) in the excited singlet state between the fluorene and the PDI and conformational relaxation within the PFP backbone [also observed for the homopolymer, poly(fluorene phenylene)]. The fast process in the (1:1) dioxane–water mixture has a time constant of 60 ps, attributed to a combination of conformational relaxation and/or singlet exciton hopping processes along the chain.^{43,71} The longest lifetime component, which dominates the decay, is clearly associated with the decay of the poly(fluorene-phenylene) relaxed structure.⁷⁹ In agreement with previous studies on related conjugated polyelectrolytes,⁸¹ the component with 100 ps lifetime found in water is attributed to copolymer aggregates (clusters) and, hence, is not observed for the copolymer in dioxane–water, a better solvent for this polymer. The dominance (in terms of amplitudes) of the two shortest components in water and of the longest components in the (1:1) dioxane–water mixture is fully consistent with the suggestions from the fluorescence quantum yield data (Table 1) that excited state quenching is a consequence of aggregation.

Femtosecond fluorescence up-conversion experiments were also performed in a (1:1) dioxane–water solution of the PBS-PFP-PDI copolymer to attempt to obtain further insight into any fast processes, such as the formation of a charge transfer (CT) or other short-lived states. However, we could not detect any fluorescence emission signal from the PDI moiety (600 nm) probably due to its ultrafast excited state decay in the

Table 2. Fluorescence Decay Times (τ_i) and Pre-Exponential Factors (a_{ij}) for the Copolymer PBS-PFP-PDI, Obtained with Excitation at 372 nm, Emission Recorded at the Wavelength Indicated in the Table, and $T = 293$ K; also Shown Is the χ^2 Value Obtained from the Analysis of the Decays

	solvent	λ_{em} (nm)	τ_1 (ns)	τ_2 (ns)	τ_3 (ns)	a_{11}	a_{12}	a_{13}	χ^2
PBS-PFP-PDI	water	420	0.01	0.10	0.70	0.915	0.063	0.022	1.10
	(1:1) dioxane–water	410	0.06		0.52	0.079		0.921	1.01
PBS-PFP	(1:1) dioxane–water	410	0.06		0.43	0.141		0.859	1.00

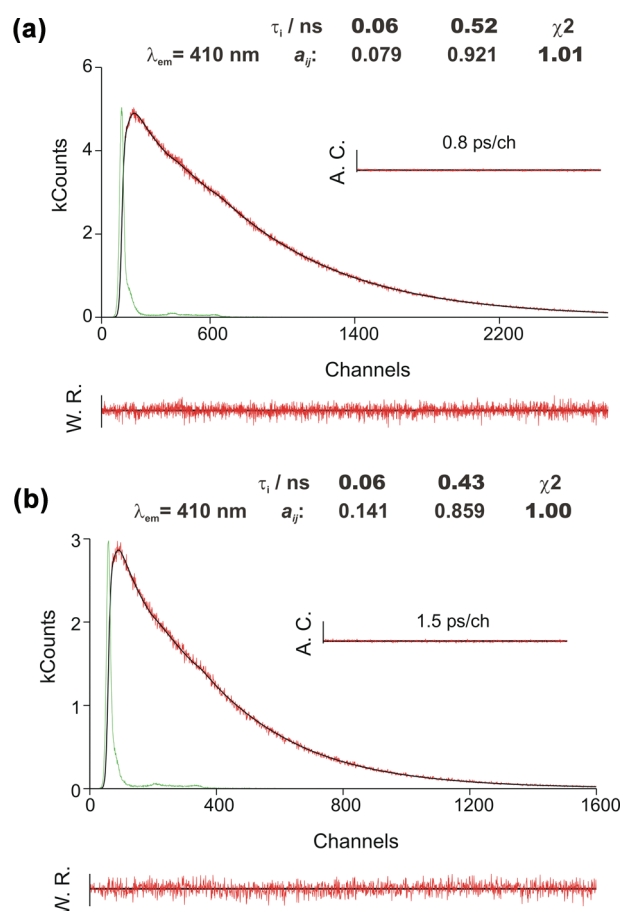


Figure 7. Fluorescence emission decay for (a) PBS-PFP-PDI and (b) PBS-PFP in the (1:1) water–dioxane mixture obtained with $\lambda_{\text{exc}} = 392$ nm and collected at $\lambda_{\text{em}} = 410$ nm. The green lines in the decays are the instrumental response function (IRF). For a better judgment of the quality of the fits, weighted residuals (W.R. scale, $-3 \leq \sigma \leq +3$), autocorrelation functions (A.C.), and chi-square values (χ^2) are also presented.

solvent used (see fs up-conversion experiments in the Supporting Information).

Fluorescence measurements can only report on the formation of emissive excited states and do not provide any information on either nonemissive excited states or any radical species formed. In polar media, it is possible that charged species may be formed in PBS-PFP-PDI after photoexcitation due to a charge transfer process. In films, this can lead to the formation of a pair of polaron-type charge states on adjacent chains.^{82–84} In solution, it is also possible to generate charged species, and the incorporation of the PDI random repeat units that have strong acceptor character may lead to formation of stable, but nonemissive, CT or radical pair states. This will alter the PBS-PFP-PDI copolymer photophysics, but these states are not necessarily observable in the TCSPC and femtosecond

fluorescence up-conversion experiments. Such nonemissive states can be studied by transient absorption measurements. Initial experiments using ns time resolution were unsuccessful, suggesting any transients formed have much shorter lifetimes. Instead, pump probe measurements with fs time resolution were performed upon exciting PBS-PFP-PDI solutions in the poly(fluorene phenylene) band at 390 nm in water and in the (1:1) water–dioxane mixture. The transient absorption spectra obtained are shown in Figure 8.

The transient absorption spectra in the two solvents [water and (1:1) water–dioxane solutions] are very similar and show two photoinduced absorption bands at 500 and 760 nm (Figure 8). In addition, there is stimulated emission at 470 nm. The longer wavelength and more intense absorption is fully formed within the time scale of the first measurement (<400 fs) and is attributed to the singlet exciton population of the phenylene-fluorene backbone (the literature value for polyfluorene excited singlet absorption is approximately 770 nm, 1.6 eV).⁸⁴ From literature data,⁷⁴ there may also be some PDI excited singlet state radical anion absorption in this region. The second broad band overlaps with the former and is centered around 500–550 nm. The kinetic results measured at 760 nm on long time scales (>10 ps) are consistent with the time constants obtained via TCSPC (see the Supporting Information). However, additional short components (0.99 ps in water and 5.7 ps in the (1:1) water–dioxane mixture) are detected, and feed the 500–550 nm photoinduced absorption band (Figure 8). A tentative assignment of this short wavelength component can be made following pulse radiolysis studies on the polymers PF2/6⁸⁵ and poly[2,7-(9,9-bis(2'-ethylhexyl)fluorene)-*alt*-1,4-phenylene] (PFP) in chloroform solutions.⁸⁶ For these systems, transient absorption spectra were observed with maxima around 540–560 nm, which were assigned unambiguously to the positively charged species (positive polarons, radical cations) of the polymers formed by one-electron oxidation reaction with the chloroform radical cation.⁸⁵ This suggests that, upon excitation of PBS-PFP-PDI in water and dioxane–water, electron (or charge) transfer occurs from the polymer backbone to the PDI unit. In contrast, if singlet excitation energy transfer would be the dominant pathway, we would expect the PFP singlet excited state to decay with formation of the excited singlet state absorption (ESA) of PDI. Furthermore, according to Janssen et al.,⁸⁷ photoinduced electron transfer is more favorable in polar solvents due to the stabilization of the charge-separated state. Hence, in water or water–cosolvent mixtures, fluorescence quenching of PFP by PDI appears to lead predominantly to electron or charge transfer. The lack of any absorption from the PDI radical anion at long time scales is surprising. It is possible that this anion radical band is spectrally shifted to the blue side in the highly polar medium, and is buried by the other signals, ground state recovery, and stimulated emission. However, a more attractive explanation, based on the known behavior of aromatic radical anions in hydroxylic solvents,⁸⁸ is that the PDI

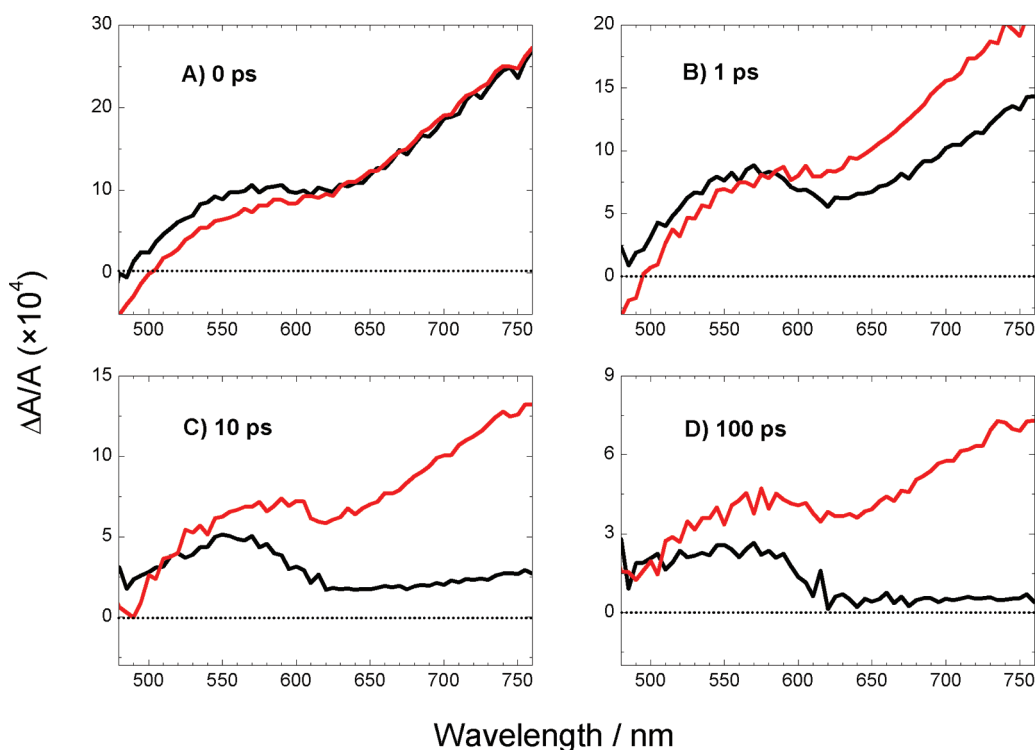


Figure 8. Evolution of the transient absorption spectra following excitation (390 nm) of PBS-PFP-PDI in water (black line) and (1:1) water–dioxane solutions (red line).

radical anion is protonated by water, leading to a short-wavelength absorbing H-atom addition product.

Further information can be obtained on the electron (charge) transfer process. Aggregation is certainly occurring in water, and there are indications from the relative amplitudes of the fast polyfluorene decay components that it may also be present in dioxane–water at the relatively high concentrations of polymer used in these experiments. It has been shown that, although organic cosolvents do help break up aggregates of conjugated polyelectrolytes, both time-resolved fluorescence and fluorescence anisotropy measurements show that aggregation does occur, even in good solvents, at high CPE concentrations.⁸⁹ We have, therefore, carried out pump–probe experiments in more dilute polymer solutions in the (1:1) dioxane–water mixture following excitation of PBS-PFP-PDI at 390 nm. Results are presented as Supporting Information. It is clear, from both spectra and kinetic traces, that there is no evidence for a long-lived state in the 500–550 nm region (Figure 9); only PFP singlet exciton photoinduced absorption is detected. The prominent subpicosecond component observed in the PFP singlet photoinduced absorption at 760 nm (too short to be detected in the TCSPC measurements) may correspond to that seen in fluorescence upconversion experiments. The remaining components are consistent with the TCSPC data. These results indicate that electron (or charge) transfer involves an interchain process.

Interaction of Cationic Surfactant CTAB with the PBS-PFP-PDI System. Since the competition between energy and electron (charge) transfer depends upon the polarity of the medium, it seemed likely that it could occur also in a more hydrophobic environment, such as has previously been seen with the PBS-PFP homopolymer in the presence of surfactants.^{90,91}

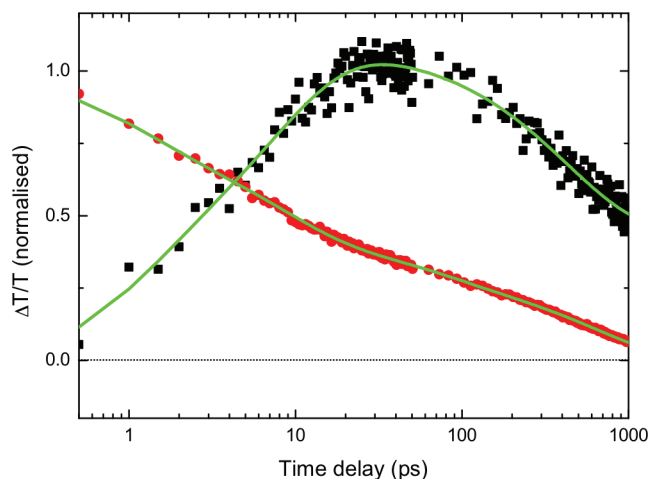


Figure 9. Global decay fit (green lines) of PBS-PFP-PDI (1:1 dioxane–water mixture) photoinduced absorption bands, 500 nm (black squares) and 760 nm (red circles).

We therefore investigated the effect of an oppositely charged surfactant on the photophysics of PBS-PFP-PDI. Various concentrations of the cationic surfactant hexadecyltrimethylammonium bromide (CTAB) were added to a solution of $\sim 5 \times 10^{-6}$ M (in terms of the copolymer repeat unit) PBS-PFP-PDI in (1:1) dioxane–water.

As was previously reported for the interaction between PBS-PFP and CTAB,³² the emission of the copolymer below the surfactant critical micelle concentration (cmc) is partially quenched. The PLQY value of 0.17 found for the PBS-PFP homopolymer/CTAB system is typical for highly aggregated systems. The surfactant induces changes of the PBS-PFP-PDI PL intensity, which is also attributed to aggregation. Above 3.4

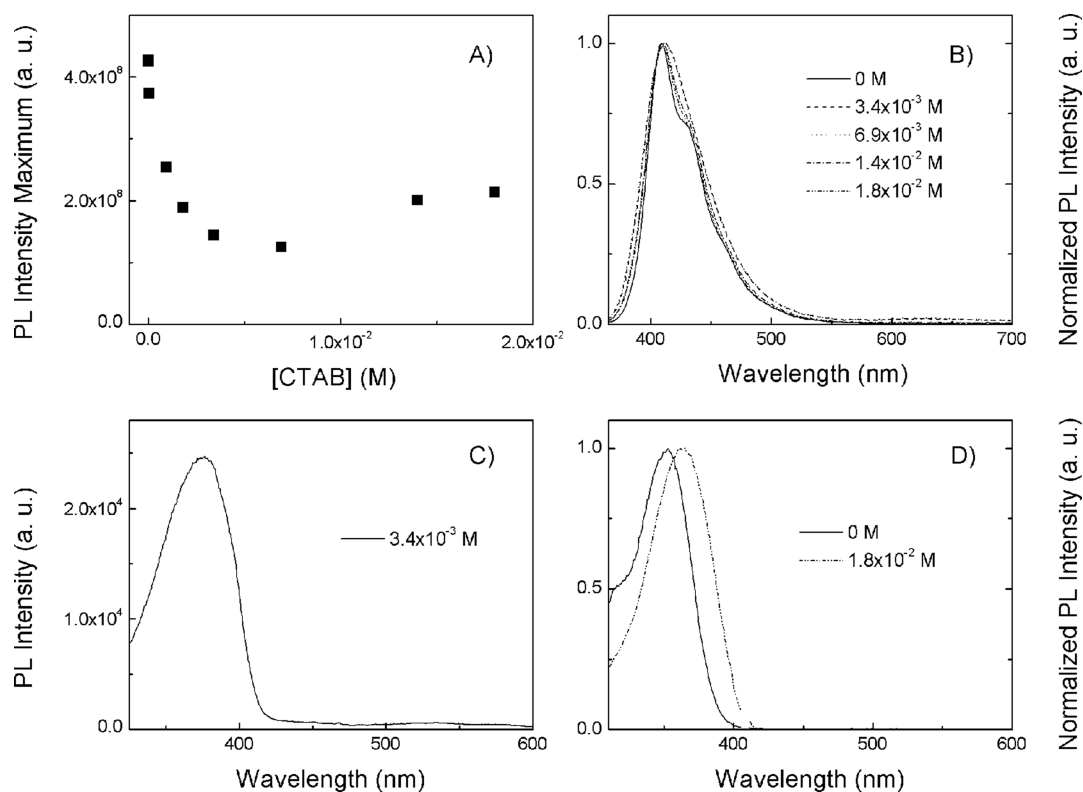


Figure 10. (A) Emission spectra of PBS-PFP-PDI $\sim 5 \times 10^{-6}$ M with increasing CTAB concentrations (M) in 50% (v/v) dioxane–water solution. (B) Normalized PBS-PFP-PDI emission spectra at concentrations above the surfactant cmc. (C) Excitation spectra of PBS-PFP-PDI $\sim 5 \times 10^{-6}$ M with 3.4 mM CTAB concentration in (1:1) dioxane–water solution with emission at the PDI 635 nm band. (D) PL excitation spectra of PBS-PFP-PDI in the absence of the surfactant and at maximum surfactant concentration, with emission at 409 nm.

mM surfactant concentration, the emission intensity increases and the vibronic structure is recovered. However, no significant shift is observed for the absorption and emission maxima (Figure 10, Table 3, and Supporting Information). The

Table 3. Absorption and Emission Maxima and Quantum Yield of PBS-PFP-PDI in (1:1) Dioxane–Water Mixture and CTAB

	0 M CTAB			1.8×10^{-2} M CTAB		
	abs. (nm)	emis. (nm)	Φ_F	abs. (nm)	emis. (nm)	Φ_F
PBS-PFP-PDI	360	408	0.55	363	409	0.47
PBS-PFP	372	410	0.52	380	416	0.17

decrease of the PLQY upon CTAB addition indicates the presence of additional excited state deactivation pathways for the PBS-PFP-PDI aggregates. There is a very weak PDI based emission in the 600–650 nm region upon excitation in the PFP band (Figure 10B and Supporting Information). This suggests that some energy transfer can occur from the PFP to the PDI

chromophore in the hydrophobic surfactant medium, as expressed by the fluorescence excitation spectra with observation at 635 nm (Figure 10 C).⁹² For a better understanding of the copolymer–surfactant system, the surfactant critical micelle concentration (cmc) was measured for the dioxane–water mixture by electrical conductivity measurements and found to be $4.0 (\pm 0.3)$ mM (see the Supporting Information), in excellent agreement with the concentration where the spectral changes in the PBS-PFP-PDI copolymer occur. The cmc is significantly higher than the cmc of CTAB in water (6.5×10^{-5} M at 25 °C).⁹³

Time-resolved fluorescence studies have also been carried out for the investigated copolymer at the maximum surfactant concentration. The decays were collected at both the polyfluorene emission maximum and within the PDI emission range and fitted in three exponentials. The results are shown in Table 4 and Figure 11.

Conjugated polyelectrolyte emission with three exponential decay components have previously been observed for related systems in the presence of polyelectrolytes, such as DNA, or surfactants.⁷⁹ The assignment of the decay time components in

Table 4. Fluorescence Decay Times (τ_i) and Pre-Exponential Factors (a_{ij}) for the Copolymer PBS-PFP-PDI and Homopolymer PBS-PFP in (1:1) Dioxane–Water with CTAB, Obtained with Excitation at 392 nm, Emission at the Wavelength Maxima, and $T = 298.15$ K; also Shown Is the χ^2 Value Obtained from the Analysis of the Decays

CTAB (18 mM)	λ_{em} (nm)	τ_1 (ns)	τ_2 (ns)	τ_3 (ns)	a_{i1}	a_{i2}	a_{i3}	χ^2
PBS-PFP	416	0.04	0.17	0.45	0.217	0.443	0.340	1.00
PBS-PFP/PDI	411	0.01	0.12	0.57	0.336	0.235	0.429	1.04
	635	0.01	0.32	1.45	0.762	0.116	0.122	1.12

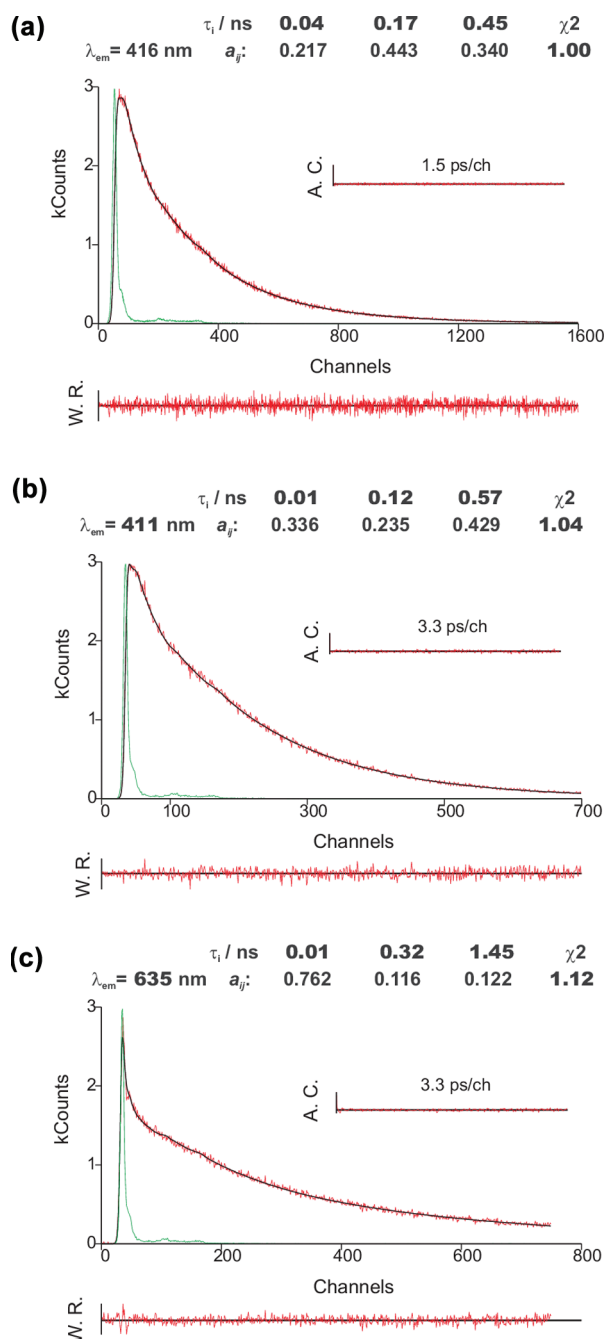


Figure 11. Fluorescence emission decay for (a) the homopolymer PBS-PFP in water–dioxane (1:1) and 18 mM CTAB obtained with $\lambda_{exc} = 392$ nm at 298 K and collected at $\lambda_{em} = 416$ nm. Fluorescence emission decays for the copolymer PBS-PFP-PDI in (1:1) water–dioxane and 18 mM CTAB obtained with $\lambda_{exc} = 392$ nm at 298.15 K and collected at (b) $\lambda_{em} = 411$ nm and (c) $\lambda_{em} = 635$ nm. The green lines in the decays are the instrumental response function (IRF). For a better judgment of the quality of the fits, weighted residuals (W.R. scale, $-3 \leq \sigma \leq +3$), autocorrelation functions (A.C.), and chi-square values (χ^2) are also presented.

such cases is not easy or even consensual. When the system is investigated in the presence of the cationic surfactant CTAB, an additional longer lifetime component (1.43 ns) is found at 635 nm in the emission range of the PDI chromophore (see the Supporting Information), indicating excitation energy transfer from the PFP backbone to PDI, possibly through an interchain pathway within the aggregates. Moreover, the shortest

component decay time for PBS-PFP-PDI in the presence of CTAB is found to decrease to a value of 10 ps.

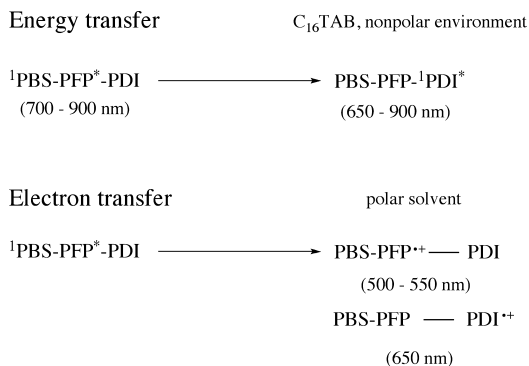
This may indicate, in contrast to the “good” solvent system dioxane–water (1:1), the presence of an additional deactivation process, such as interchain energy hopping, competing with conformational relaxation (CR) and on-chain excitation energy transfer (ET). These results are all in agreement with the surfactant inducing aggregation of the CPE. Comparable decay components (ca. 0.32 and 1.43 ns) have previously been reported by Fron et al.⁴⁵ for a nonionic PF copolymer with random on-chain PDI chromophores in polar solvents. The authors suggested the occurrence of a photoinduced charge transfer (CT) process. The decay time observed in the region of the PDI emission (1.43 ns) is considerably shorter than that of the isolated chromophore (5.65 ns), suggesting a competing deactivation process, which may involve charge transfer.

CONCLUSIONS

An anionic conjugated polyelectrolyte (CPE) composed of phenylene-*alt*-fluorene repeat units and randomly distributed perylene diimide (PDI) on-chain chromophores has been synthesized and its photophysical behavior studied in various media. The optical spectra of the copolymer in water and dioxane–water mixtures showed no significant emission component from the PDI chromophore. However, single chain wide field imaging in PVA films confirmed incorporation of the PDI dye within the PFP polymer chain, although at low percentage. Time-resolved PL, femtosecond fluorescence, and transient absorption experiments in water and dioxane–water solution document the presence of fast PL decay components and suggest that there is an efficient nonradiative decay pathway in this system, that involves electron (or charge) transfer leading to quenching of both the PFP and PDI emission. Therefore, the effect of adding the oppositely charged cationic surfactant leads to the weak long wavelength PDI-based PL component being seen. Low efficiency energy transfer is only observed in a nonpolar environment where the cationic CTAB molecules shield the copolymer for water, forming surfactant + polyelectrolyte complexes.

In summary on all the above data, both energy and electron (or charge) transfer are possible with PBS-PFP-PDI upon excitation of the PFP copolymer units. The kinetic pathways, depicted in Scheme 1, show this can be mediated by control of the polarity of the environment through use of surfactants.

Scheme 1. Schematic Kinetic Pathway for PBS-PFP-PDI in Water, (1:1) Water–Dioxane, and Cationic Surfactant CTAB upon Excitation of the PFP Unit



■ ASSOCIATED CONTENT

● Supporting Information

Additional figures and table related to the critical micelle concentration of CTAB in a 50% dioxane–water solution, the energy transfer process in the PBS-PFP-PDI copolymer, TC-SPC measurements of the PBS-PFP-PDI copolymer, emission spectra of the PBS-PFP-PDI in the presence of CTAB, femtosecond fluorescence up-conversion experiments, and pump–probe experiments. This material is available free of charge via the Internet at <http://pubs.acs.org>.

■ AUTHOR INFORMATION

Corresponding Author

*E-mail: anatmarques@qui.uc.pt.

Notes

The authors declare no competing financial interest.

■ ACKNOWLEDGMENTS

The authors are grateful to Professor Klaus Müllen (Max Planck Institute for Polymer Research) for supplying the PDI monomer, Dr. Ana Borba (University of Coimbra) for the FTIR measurements, and Dr. João Pina (University of Coimbra) for assistance and valuable ideas on the time-resolved fluorescence procedure. A.T.M. and L.L.G.J. acknowledge Fundação para a Ciência e a Tecnologia (FCT), of the Portuguese Ministry for Science, Technology and Higher Education, for the doctoral grant SFRH/BD/36666/2007 and postdoctoral grant SFRH/BPD/26415/2006, respectively. L.L.G.J. thanks Laboratório de Computação Avançada, of the Department of Physics of the University of Coimbra, for the computing facilities (Milipeia Cluster). J.H., E.F. and S.R. acknowledge financial support from the Research Foundation Flanders (FWO Grants G.0402.09 G.0413.10 G.0181.10), the K.U.Leuven Research Fund (GOA2006/2, the Flemish Government (long term structural funding- Methusalem funding CASAS), the Federal Science Policy of Belgium (IAP-VI/27), and the Hercules foundation (HER/08/021).

■ REFERENCES

- (1) Liu, B.; Bazan, G. C. *Chem. Mater.* **2004**, *16*, 4467.
- (2) Jiang, H.; Taranekar, P.; Reynolds, J. R.; Schanze, K. S. *Angew. Chem., Int. Ed.* **2009**, *48*, 4300.
- (3) Hoven, C. V.; Garcia, A.; Bazan, G. C.; Nguyen, T.-Q. *Adv. Mater.* **2008**, *20*, 3793.
- (4) Pinto, M. R.; Schanze, K. S. *Synthesis* **2002**, *9*, 1293.
- (5) Gans, B.-J.; de; Duineveld, P. C.; Schubert, U. S. *Adv. Mater.* **2004**, *16*, 203.
- (6) Wallikewitz, B. H.; de la Rosa, M.; Kremer, J. H.-W. M.; Hertel, D.; Meerholz, K. *Adv. Mater.* **2010**, *22*, 531.
- (7) Pei, Q. B.; Yu, G.; Zhang, C.; Yang, Y.; Heeger, A. J. *Science* **1995**, *269*, 1086.
- (8) Huang, F.; Wu, H.; Wang, D.; Yang, W.; Cao, Y. *Chem. Mater.* **2004**, *16*, 708.
- (9) Edman, L.; Pauchard, M.; Liu, B.; Bazan, G.; Moses, D.; Heeger, A. J. *Appl. Phys. Lett.* **2003**, *82*, 3961.
- (10) Ortony, J. H.; Yang, R.; Brzezinski, J. Z.; Edman, L.; Nguyen, T.-Q.; Bazan, G. C. *Adv. Mater.* **2008**, *20*, 298.
- (11) Pu, K.-Y.; Li, K.; Liu, B. *Adv. Funct. Mater.* **2010**, *20*, 2770.
- (12) Tapia, M. J.; Montserín, M.; Valente, A. J. M.; Burrows, H. D.; Mallavia, R. *Adv. Colloid Interface Sci.* **2010**, *158*, 94.
- (13) Pu, K.-Y.; Liu, B. *Adv. Funct. Mater.* **2009**, *19*, 277.
- (14) Duarte, A.; Pu, K.-Y.; Liu, B.; Bazan, G. C. *Chem. Mater.* **2011**, *23*, 501.
- (15) Wang, C.; Zhan, R.; Pu, K.-Y.; Liu, B. *Adv. Funct. Mater.* **2010**, *20*, 2597.
- (16) Li, K.; Liu, B. *Polym. Chem.* **2010**, *1*, 252.
- (17) Duan, X.; Liu, L.; Feng, X.; Shu Wang, S. *Adv. Mater.* **2010**, *22*, 1.
- (18) Fang, J.; Wallikewitz, B. H.; Gao, F.; Tu, G.; Müller, C.; Pace, G.; Friend, R. H.; Huck, W. T. S. *J. Am. Chem. Soc.* **2011**, *133*, 683.
- (19) Hoven, C. V.; Wang, H.; Elbing, M.; Garner, L.; Winkelhaus, D.; Bazan, G. C. *Nat. Mater.* **2010**, *9*, 249.
- (20) Seo, J. H.; Gutacker, A.; Walker, B.; Cho, S.; Garcia, A.; Yang, R.; Nguyen, T.-Q.; Heeger, A. J.; Bazan, G. C. *J. Am. Chem. Soc.* **2009**, *131*, 18220.
- (21) Taranekar, P.; Qiao, Q.; Jiang, H.; Ghiviriga, I.; Schanze, K. S.; Reynolds, J. R. *J. Am. Chem. Soc.* **2007**, *129*, 8958.
- (22) Oh, S.-H.; Na, S.-I.; Jo, J.; Lim, B.; Vak, D.; Kim, D.-Y. *Adv. Funct. Mater.* **2010**, *20*, 1.
- (23) Xing, C.; Liu, L.; Shi, Z.; Li, Y.; Wang, S. *Adv. Funct. Mater.* **2010**, *20*, 2175.
- (24) Moons, E. J. *Phys.: Condens. Matter* **2002**, *14*, 12235.
- (25) Schwartz, B. J. *Annu. Rev. Phys. Chem.* **2003**, *54*, 141.
- (26) Veldman, D.; Bastiaansen, J. J. A. M.; Langeveld-Voss, B. M. W.; Sweelssen, J.; Koetse, M. M.; Meskers, S. C. J.; Janssen, R. A. J. *Thin Solid Films* **2006**, *511–512*, 581.
- (27) Wågberg, T.; Liu, B.; Orädd, G.; Eliasson, B.; Edman, L. *Eur. Polym. J.* **2009**, *45*, 3230.
- (28) Montserín, M.; Tapia, M. J.; Ribeiro, A. C. F.; Santos, C. I. A. V.; Valente, A. J. M.; Burrows, H. D.; Mallavia, R.; Nilsson, M.; Söderman, O. *J. Chem. Eng. Data* **2010**, *55*, 1860.
- (29) Tapia, M. J.; Montserín, M.; Costoyas, A.; Burrows, H. D.; Marques, A. T.; Pais, A. A. C. C.; Valente, A. J. M.; R. Mallavia, R.; Scherf, U.; Pinazo, A.; Pérez, L.; Morán, M. C. *J. Mol. Liq.* **2010**, *156*, 18.
- (30) Montserín, M.; Burrows, H. D.; Mallavia, R.; Paolo, R. E. D.; Maçanita, A. L.; Tapia, M. J. *Langmuir* **2010**, *26*, 11705.
- (31) Fonseca, S. M.; M. Eusébio, M. E.; Castro, R.; Burrows, H. D.; Tapia, M. J.; Olsson, U. *J. Colloid Interface Sci.* **2007**, *315*, 805.
- (32) Tapia, M. J.; Burrows, H. D.; Valente, A. J. M.; Pradhan, S.; Scherf, U.; Lobo, V. M. M.; Pina, J.; Seixas de Melo, J. S. *J. Phys. Chem. B* **2005**, *109*, 19108.
- (33) Chen, L.; Xu, S.; McBranch, D.; Whitten, D. J. *Am. Chem. Soc.* **2000**, *122*, 9302.
- (34) Jaiser, F.; Neher, D.; Meisel, A.; Nothofer, H.-G.; Miteva, T.; Herrmann, A.; Müllen, K.; Scherf, U. *J. Chem. Phys.* **2008**, *129*, 114901.
- (35) Hofkens, J.; Cotlet, M.; Vosch, T.; Tinnfeld, P.; Weston, K. D.; Ego, C.; Grimsdale, A.; Müllen, K.; Beljonne, D.; Brédas, J. L.; Jördens, S.; Schweitzer, G.; Sauer, M.; De Schryver, F. *Proc. Natl. Acad. Sci. U.S.A.* **2003**, *100*, 13146.
- (36) Gomez, R.; Seoane, C.; Segura, J. L. *J. Org. Chem.* **2010**, *75*, 5099.
- (37) Ego, C.; Marsitzky, D.; Becker, S.; Zhang, J.; Grimsdale, A. C.; Müllen, K.; MacKenzie, D.; Silva, C.; Friend, R. H. *J. Am. Chem. Soc.* **2003**, *125*, 437.
- (38) Marques, A. T.; Pinto, S. M. A.; Monteiro, C. J. P.; Seixas de Melo, J. S.; Burrows, H. D.; Scherf, U.; Calvete, M. J. F.; Mariette M. Pereira, M. M. *J. Polym. Sci., Part A: Polym. Chem.* **2012**, *50*, 1408.
- (39) Weil, T.; Vosch, T.; Hofkens, J.; Peneva, K.; Müllen, K. *Angew. Chem., Int. Ed.* **2010**, *49*, 9068.
- (40) Yuan, Z.; Li, J.; Xiao, Y.; Li, Z.; Qian, X. *J. Org. Chem.* **2010**, *75*, 3007.
- (41) Kircher, T.; Löhmannsröben, H.-G. *Phys. Chem. Chem. Phys.* **1999**, *1*, 3987.
- (42) De Schryver, F. C.; Vosch, T.; M. Cotlet, M.; Van Der Auweraer, M.; Müllen, K.; Hofkens, J. *Acc. Chem. Res.* **2005**, *38*, 514.
- (43) Fron, E.; Schweitzer, G.; Jacob, J.; Van Vooren, A. V.; Beljonne, D.; Müllen, K.; Hofkens, J.; Van der Auweraer, M.; De Schryver, F. C. *ChemPhysChem* **2007**, *8*, 1386.
- (44) Dias, F. B.; Knaapila, M.; Monkman, A. P.; Burrows, H. D. *Macromolecules* **2006**, *39*, 1598.

- (45) Fron, E.; Deres, A.; Rocha, S.; Zhou, G.; Müllen, K.; De Schryver, F. C.; Sliwa, M.; Hiroshi, U.; Hofkens, J.; Vosch, T. *J. Phys. Chem. B* **2010**, *114*, 1277.
- (46) List, E. J. W.; Creely, C.; Leising, G.; Schulte, N.; Schluter, A. D.; Scherf, U.; Müllen, K.; Graupner, W. *Chem. Phys. Lett.* **2000**, *325*, 132.
- (47) Stevens, M. A.; Silva, C.; Russel, D. M. N.; Friend, R. H. *Phys. Rev. B* **2001**, *63*, 165213.
- (48) Romanovskii, Y. V.; Bassler, H.; Scherf, U. *Chem. Phys.* **2002**, *276*, 321.
- (49) Förster, T. *Discuss. Faraday Soc.* **1959**, *27*, 7.
- (50) Förster, T. *Ann. Phys.* **1948**, *2*, 55.
- (51) Burrows, H. D.; Lobo, V. M. M.; Pina, P.; Ramos, M. L.; Seixas de Melo, J. S.; Valente, A. J. M.; Tapia, M. J.; Pradhan, S.; Scherf, U. *Macromolecules* **2004**, *37*, 7425.
- (52) Nefedov, P. P.; Lazareva, M. A.; Belenkii, B. G.; Frenkel, S. Y.; Koton, M. M. *J. Chromatogr.* **1979**, *170*, 11.
- (53) Montalti, M.; Credi, A.; Prodi, L.; Gandolfi, M. T. *Handbook of Photochemistry 3rd Ed.*; Taylor & Francis: New York, 2006.
- (54) Seixas de Melo, J. *Chem. Educ.* **2005**, *10*, 29.
- (55) Seixas de Melo, J.; Fernandes, P. F. *J. Mol. Struct.* **2001**, *69*, 565.
- (56) Pina, J.; Seixas de Melo, J. S.; Burrows, H. D.; Maçanita, A. L.; Galbrecht, F.; Bünnagel, T.; Scherf, U. *Macromolecules* **2009**, *42*, 1710.
- (57) Boens, N.; Qin, W.; Basarić, N.; Hofkens, J.; Ameloot, M.; Pouget, J.; Lefèvre, J.-P.; Valeur, B.; Gratton, E.; vandeVen, M.; Silva, N. D.; Engelborghs, Y.; Willaert, K.; Sillen, A.; Rumbles, G.; Phillips, D.; Visser, A. J. W. G.; Hoek, A. V.; Lakowicz, J. R.; Malak, H.; Gryczynski, L.; Szabo, A. G.; Krajcarski, D. T.; Tamai, N.; Miura, A. *Anal. Chem.* **2007**, *79*, 2137.
- (58) Striker, G.; Subramaniam, V.; Seidel, C. A. M.; Volkmer, A. *J. Phys. Chem. B* **1999**, *103*, 8612–8617.
- (59) Schmidt, M. W.; Baldrige, K. K.; Boatz, J. A.; Elbert, S. T.; Gordon, M. S.; Jensen, J. H.; Koseki, S.; Matsunaga, N.; Nguyen, K. A.; Su, S. J.; Windus, T. L.; Dupuis, M.; Montgomery, J. A. *J. Comput. Chem.* **1993**, *14*, 1347.
- (60) Becke, A. D. *J. Chem. Phys.* **1993**, *98*, 5648.
- (61) Lee, C.; Yang, W.; Parr, R. G. *Phys. Rev. B* **1988**, *37*, 785.
- (62) Burrows, H. D.; Fonseca, S. M.; Silva, C. L.; Pais, A. C. C.; Tapia, M. J.; Pradhan, S.; Scherf, U. *Phys. Chem. Chem. Phys.* **2008**, *10*, 4420.
- (63) Gutacker, A.; Adamczyk, S.; Helfer, A.; Garner, L. E.; Evans, R. C.; Fonseca, S. M.; Knaapila, M.; Bazan, G. C.; Burrows, H. D.; Scherf, U. *J. Mater. Chem.* **2010**, *20*, 1423.
- (64) Holman, M. W.; Liu, R.; Zang, L.; Yan, P.; DiBenedetto, S. A.; Bowers, R. D.; Adams, D. M. *J. Am. Chem. Soc.* **2004**, *126*, 16126.
- (65) Margineanu, A.; Hofkens, J.; Cotlet, M.; Habuchi, S.; Stefan, A.; Qu, J.; Kohl, C.; Müllen, K.; Vercammen, J.; Engelborghs, Y.; Gensch, T.; De Schryver, F. C. *J. Phys. Chem. B* **2004**, *108*, 12242.
- (66) Burrows, H. D.; Knaapila, M.; Fonseca, S. M.; Costa, T. In *Conjugated Polyelectrolytes. Fundamentals and Applications in Emerging Technologies*; Liu, B.; Bazan, G. C., Eds.; Wiley, in press.
- (67) Beljonne, D.; Pourtois, G.; Hennebicq, E.; Herz, L. M.; Friend, R. H.; Scholes, G. D.; Setayeshi, S.; Müllen, K.; Brédas, J. L. *Proc. Natl. Acad. Sci. U.S.A.* **2002**, *99*, 10982.
- (68) Turro, N. J. *Modern Molecular Photochemistry*; University Science Books: Sausalito, CA, 1991.
- (69) Lakowicz, J. R. *Principles of Fluorescence Spectroscopy*, 3rd ed.; Springer: New York, 2006.
- (70) Burrows, H. D.; Fonseca, S. M.; Dias, F. B.; Seixas de Melo, J. S.; de; Monkman, A. P.; Scherf, U.; Pradhan, S. *Adv. Mater.* **2009**, *21*, 1155.
- (71) Pinto, S. M.; Burrows, H. D.; Pereira, M. M.; Fonseca, S. M.; B. Dias, F. B.; Mallavia, R.; Tapia, M. J. *J. Phys. Chem. B* **2009**, *113*, 16093.
- (72) Morgado, J.; Cacialli, F.; Iqbal, R.; Moratti, S. C.; Holmes, A. B.; Yahsioglu, G.; Milgrom, L. R.; Friend, R. H. *J. Mater. Chem.* **2001**, *11*, 278.
- (73) Dedecker, P.; Muls, B.; Deres, A.; Uji-i, H.; Hotta, J.; Sliwa, M.; Soumillion, J.-P.; Müllen, K.; Enderlein, J.; Hofkens, J. *Adv. Mater.* **2009**, *21*, 1079.
- (74) Delport, F.; Deres, A.; Hotta, J.-i.; Pollet, J.; Verbruggen, B.; Sels, B.; Hofkens, J.; Lammertyn, J. *Langmuir* **2010**, *26*, 1594.
- (75) Becker, K.; Lupton, J. M. *J. Am. Chem. Soc.* **2006**, *128*, 6468.
- (76) Lin, H.; Tabaei, S. R.; Thomsson, D.; Mirzov, O.; Larsson, P.-O.; Scheblykin, I. G. *J. Am. Chem. Soc.* **2008**, *130*, 7042.
- (77) Onda, S.; Kobayashi, H.; Hatano, T.; Furumaki, S.; Habuchi, S.; Vacha, M. *J. Phys. Chem. Lett.* **2011**, *2*, 2827.
- (78) Flors, C.; Oesterling, I.; Schnitzler, T.; Fron, E.; Schweitzer, G.; Sliwa, M.; Herrmann, A.; Auweraer, M. van der; Schryver, F. C. de; Müllen, K.; Hofkens, J. *J. Phys. Chem. C* **2007**, *111*, 4861.
- (79) Montserratín, M.; Burrows, H. D.; Valente, A. J. M.; Lobo, V. M. M.; Mallavia, R.; Tapia, M. J.; García-Zubiri, I. X.; Di Paolo, R. E.; Maçanita, A. L. *J. Phys. Chem. B* **2007**, *111*, 13560.
- (80) Dias, F. B.; Maçanita, A. L.; Seixas de Melo, J. S.; Burrows, H. D.; Guntner, R.; Scherf, U.; Monkman, A. P. *J. Chem. Phys.* **2003**, *118*, 7119.
- (81) Al Attar, H. A.; Monkman, A. P. *Adv. Funct. Mater.* **2008**, *18*, 2498.
- (82) Kersting, R.; Lemmer, U.; Deussen, M.; Bakker, H. J.; Mahrt, R. F.; Kurz, H.; Arkhipov, V. I.; Bassler, H.; Gobel, E. O. *Phys. Rev. Lett.* **1994**, *73*, 1440.
- (83) Conwell, E. M.; Mizes, H. A. *Phys. Rev. B* **1995**, *51*, 6953.
- (84) Monkman, A.; Rothe, C.; King, S.; Dias, F. *Advances in Polymer Science*; Springer-Verlag: Berlin, Heidelberg, 2008.
- (85) Burrows, H. D.; Seixas de Melo, J. S.; Forster, M.; Güntner, R.; Scherf, U.; Monkman, A. P.; Navaratnam, S. *Chem. Phys. Lett.* **2004**, *385*, 105.
- (86) Fratilou, S.; Fonseca, S. M.; Grozema, F. C.; Burrows, H. D.; Costa, M. L.; Charas, A.; Morgado, J.; Siebbeles, L. D. A. *J. Phys. Chem. C* **2007**, *111*, 5812.
- (87) Neuteboom, E. E.; Meskers, S. C. J.; Beckers, E. H. A.; Chopin, S.; Janssen, R. A. J. *J. Phys. Chem. A* **2006**, *110*, 12363.
- (88) Dorfman, K. *Acc. Chem. Res.* **1970**, *3*, 224.
- (89) Davies, M. L.; Douglas, P.; Burrows, H. D.; da G. Miguel, M.; Douglas, A. *J. Phys. Chem. B* **2011**, *115*, 6885.
- (90) Knaapila, M.; Almásy, L.; Garamus, V. M.; Pearson, C.; Pradhan, S.; Petty, M. C.; Scherf, U.; Burrows, H. D.; Monkman, A. P. *J. Phys. Chem. B* **2006**, *110*, 10248.
- (91) Burrows, H. D.; Tapia, M. J.; Fonseca, S. M.; Pradhan, S.; Scherf, U.; Silva, C. L.; Pais, A. A. C. C.; Valente, A. J. M.; Schillén, K.; Alfredsson, V.; Carnerup, A. M.; Matija Tomsic, M.; Jamnik, A. *Langmuir* **2009**, *25*, 5545.
- (92) Feist, F. A.; Zickler, M. F.; Basché, T. *ChemPhysChem*, **2012**, *12*, 1499.
- (93) Mukerjee, P.; Mysels, K. J. *Critical Micelle Concentration of Aqueous Surfactant Systems*; National Bureau of Standards: Washington, DC, 1971.

NOTE ADDED AFTER ASAP PUBLICATION

This paper was published ASAP on June 18, 2012. An abstract graphic was added. The revised paper was reposted on June 28, 2012.